Extreme precipitation in the Netherlands: An event attribution case study

Jonathan M Eden, Sarah F Kew, Omar Bellprat, Geert Lenderink, Iris Manola, Hiba Omrani, Geert Jan van Oldenborgh

Weather and Climate Extremes 21 (2018) 90–101

Contents lists available at ScienceDirect

Weather and Climate Extremes

journal homepage: www.elsevier.com/locate/wace

Extreme precipitation in the Netherlands: An event attribution case study

Jonathan M. Eden[a,b,*], Sarah F. Kew[b], Omar Bellprat[c], Geert Lenderink[b], Iris Manola[d], Hiba Omrani[e], Geert Jan van Oldenborgh[b]

[a] Centre for Agroecology, Water and Resilience, Coventry University, UK
[b] Royal Netherlands Meteorological Institute (KNMI), De Bilt, Netherlands
[c] Barcelona Supercomputing Center, Barcelona, Spain
[d] Department of Environmental Sciences, Wageningen University, Netherlands
[e] Laboratoire des Sciences du Climat et de l'Environnement, Gif sur-Yvette, France

A B S T R A C T

Attributing the change in likelihood of extreme weather events, particularly those occurring at small spatiotemporal scales, to anthropogenic forcing is a key challenge in climate science. While a warmer world is associated with an increase in atmospheric moisture on a global scale, the impact on the magnitude of extreme precipitation episodes has substantial regional variability. Analysis of individual cases is important in understanding the extent of these changes on spatial scales relevant to stakeholders.

Here, we present a probabilistic attribution analysis of the extreme precipitation that fell in large parts of the Netherlands on 28 July 2014. Using a step-by-step approach, we aim to identify changes in intensity and likelihood of such an event as a result of anthropogenic global warming while highlighting the challenges in performing robust event attribution on high-impact precipitation events that occur at small scales. A method based on extreme value theory is applied to observational data in addition to global and regional climate model ensembles that pass a robust model evaluation process. Results based on observations suggest a strong and significant increase in the intensity and frequency of a 2014-type event as a result of anthropogenic climate change but trends in the model ensembles used are considerably smaller. Our results are communicated alongside considerable uncertainty, highlighting the difficulty in attributing events of this nature. Application of our approach to convection-resolving models may produce a more robust attribution.

1. Introduction

It is widely acknowledged that changes in the magnitude and frequency of extreme events are among the main consequences of a changing climate (Hartmann et al., 2013). Conversely, weather and climate extremes associated with substantial impacts are often followed by questions from stakeholders and the media about the role played by anthropogenic climate change. The attribution of extreme events, either recent or in the historical record, to anthropogenic activities or a mode of the natural variability of the climate system (e.g. El Niño Southern Oscillation) is important in understanding and communicating how the risk of such events will change in the future. However, quantifying changes in the likelihood of events that are rare by definition is not straightforward. As a result, there are many challenges in the field of event attribution in terms of event definition, conducting the analysis itself and in communicating the resultant findings to stakeholders and decision-makers in the most effective way (Stott et al., 2016).

While there is a reasonable degree of consensus on the attribution of daily temperature extremes to anthropogenic climate change (National Academies of Sciences, Engineering, and Medicine, 2016), there is far less agreement with regard to other extreme events, including episodes of extreme precipitation (e.g. Kay et al., 2011; van Oldenborgh et al., 2012; Schaller et al., 2014; Vautard et al., 2015; Eden et al., 2016; Van Oldenborgh et al., 2016; Otto et al., 2018). A possible increase in extreme precipitation follows from the increase in moisture in the atmosphere that is predicted by the Clausius-Clapeyron (CC) relation for constant relative humidity. On a global scale, observations show that the increase in moisture in an atmosphere warmer than a century ago is broadly in line with the CC relation of approximately 6–7% per K (Hartmann et al., 2013), and that relative humidity is fairly constant. However, on smaller temporal and spatial scales, rates of extreme precipitation are influenced to a greater extent by atmospheric circulation and vertical stability in addition to local moisture availability (Berg et al., 2009; Hoerling et al., 2014; Lenderink et al., 2017). Many of these processes and other features of extreme precipitation events are not sufficiently represented in climate model simulations and limited station networks mean that many short-term convective events are not accurately represented in the observational data. Therefore, when conducting an analysis on precipitation events of this nature, both observational data and model simulations must be used with caution.

One such short-term convective precipitation event occurred in the Netherlands on 28 July 2014 when a number of thunderstorms moved

* Corresponding author. Centre for Agroecology, Water and Resilience (CAWR), Coventry University, Ryton Gardens, Warwickshire, CV8 3LG, UK.
E-mail address: jonathan.eden@coventry.ac.uk (J.M. Eden).

https://doi.org/10.1016/j.wace.2018.07.003
Received 17 November 2017; Received in revised form 16 July 2018; Accepted 20 July 2018
Available online 30 July 2018

across the country. Precipitation totals in excess of 130 mm fell in just a few hours leading to localised flooding, €10 m property damage in the Netherlands (the same complex caused further damage in Belgium) and widespread traffic disruption. Given the acute nature of this type of event, the consequent impacts are often accompanied by questions within the media and wider public about the role played by anthropogenic climate change in the event's occurrence and magnitude.

Here, we outline and implement a systematic probabilistic attribution analysis of the 28 July 2014 episode of extreme precipitation using observation- and climate model-based methodologies. Consideration is given to the present challenges in event attribution and the steps required to establish and communicate a robust statement about the likelihood of this and similar events as a result of anthropogenic climate change. These include the following: delineating the event and its impacts (Section 2); framing the attribution question and establishing a definition of the event to be used in the analysis (Section 3); evaluating the exceptionality of the event and detection of changes in the frequency and magnitude of related extremes in observations (Section 4); using climate model simulations that pass appropriate evaluation (Section 5) to attribute any such changes to anthropogenic activities (Section 6).

2. Event background

2.1. Observational analysis

During the morning of 28 July 2014 a complex system of severe thunderstorms entered the Netherlands from Belgium. Intense episodes of precipitation and subsequent flooding resulted in numerous impacts throughout the country including the closure of major highways, flight cancellations, widespread property damage and agricultural losses due to the flooding of low-lying polders (https://www.rainproof.nl/wolkbreuk-28-juli). Total damages in the Netherlands were estimated to be at least €10 m.

We used three sources of observations of the event: (i) 31 automatic weather stations (AWS) that record 10-min precipitation, summed to 0–24 UTC daily totals; (ii) 324 volunteer manual stations that record 8-8 UTC totals only, of which 102 have been homogenised back to 1910, and 240 back to 1951[1] (Buishand et al., 2013); (iii) radar data since 2008, calibrated to the above rain gauges. Radar observations of daily precipitation totals (0–24 UTC) are shown in Fig. 1a for 28 July 2014. Fig. 1b shows the totals of the 28 and 29 July 8–8 UTC accumulations, which capture the whole event. Sub-daily resolution radar observations reveal that the main cluster moved in during the night and early morning in a north-northwest direction. Heavy precipitation fell in the western half of the Netherlands during the morning and later along a band of thunderstorms extending from the coast eastwards across the centre of the country. An observed total of 131.6 mm at the AWS at the airfield of Deelen (52°03′ N, 5°52′ E) amounted to the highest gauge value in any part of the Netherlands on that day. The most intense precipitation instances were associated with a spatial dimension of only a few kilometres and therefore not fully captured by gauge observations. An additional problem was that the complex passed many areas around 08:00 UTC, so that the precipitation in the dense volunteer network of 8-8 UTC gauges was split over two days.

To further understand the extent to which the 28 July 2014 event was exceptional, we explore the prevailing synoptic situation and the origin of the moisture contribution to the thunderstorms. The days preceding the event were characterised by one area of high pressure over the eastern Atlantic, which remained quasi-stationary, and another area of high pressure situated over Scandinavia coupled with a region of lower pressure over central Europe (Fig. 1c). This north-south pressure dipole gave rise to easterly flow over the Baltic region, across the Netherlands towards the UK, and acted to block a westerly flow across the Atlantic. The area of high pressure over Scandinavia was also associated with anomalously high temperatures (Fig. 1d) and led to higher rates of evaporation over the Baltic. Some isolated convective activity over the Netherlands was already present during this period. Two subsequent developments (27–28 July) increased atmospheric instability. The stabilising Scandinavian high moved away to the east, and a mid-tropospheric cold low approached, moving quickly southeastward over the UK. The low was accompanied on its eastern side by a surface convergence line and cold front. The low's associated circulation also brought a plume of moist air from the south on its eastern side at mid-tropospheric levels, which in the ERA-interim reanalysis coincided with a mesoscale region of strong ascent close to where the storms developed.

The measure CAPE (convective available potential energy), gives an indication of the inherent instability of the atmospheric profile to convection. Unfortunately there are no suitable observed (radiosonde) profiles for this event. Instead, we calculated CAPE by taking a surface parcel initialised with surface observations but using simulated profiles of the regional model KNMI-RACMO (Meijgaard et al., 2008; Meijgaard et al., 2012, also used below in Sections 2.2 and 5, but here using the hindcast run of 38 h, driven by ERA-interim and starting at 12:00; see Loriaux et al., 2016). Instead of a typical summer situation with a convective boundary layer topped with cumulus, we find that surrounding the time of the event, the near surface is already close to saturation. The CAPE values, of order 1000 J, are high but not exceptionally so given the high surface dewpoint, so the atmosphere was not very unstable due to comparatively low surface temperatures.

In summary, the synoptic picture suggests that moisture may have been transported into the vicinity of the event from the Baltic and also from a southerly ‘warm conveyor belt', with moisture possibly originating from the Atlantic. Further insight is required into the origin of the convective instability.

2.2. Moisture source and transport

The synoptic situation provides an approximation for the source and transport of moisture but much more detailed insight can be gained from trajectory analysis. A trajectory algorithm was applied to meteorological fields from the ERA-interim reanalysis (Dee et al., 2011) following a two-dimensional Lagrangian method (Dominguez et al., 2006; van den Hurk and van Meijgaard, 2010). While the resolution of ERA-interim is too coarse for resolving the convective storms associated with the 28 July 2014 event, the spatial extent of large-scale precipitation is reasonably well-captured (not shown) and therefore we assume the same for large-scale moisture transport. The highest precipitation values are actually placed to the west in the North Sea but as there is no suggestion that this is a result of systematic bias, our analysis considered sources of moisture for precipitation falling in the position of the observed maxima. For each grid point within the predefined target region (4°E − 7°E, 53°N-51°N), a trajectory was determined for each of four analysis times during 28 July 2014 (0000, 0600, 1200 and 1800 UTC) for which precipitation > 1 mm was recorded in ERA-interim. The product of the atmospheric moisture content and horizontal wind was vertically integrated to construct a sequence of upstream atmospheric columns over the preceding five-day period. Cumulative evaporation and precipitation are calculated at each grid point passed by a trajectory and expressed as a contribution to the total diagnosed precipitation within the target region. For comparison, back trajectories were determined for all July precipitation between 1979 and 2014 and a subset of the 50 most severe one-day events.

Moisture for precipitation during July is typically maritime in origin: the key regions of net moisture gain were found to be the western North Atlantic and the English Channel (Fig. 2a). Trajectories

[1] The second data source has been corrected to first order for a recently discovered manufacturing problem in the rain gauges by a bias correction that increases linearly from zero to −6%.

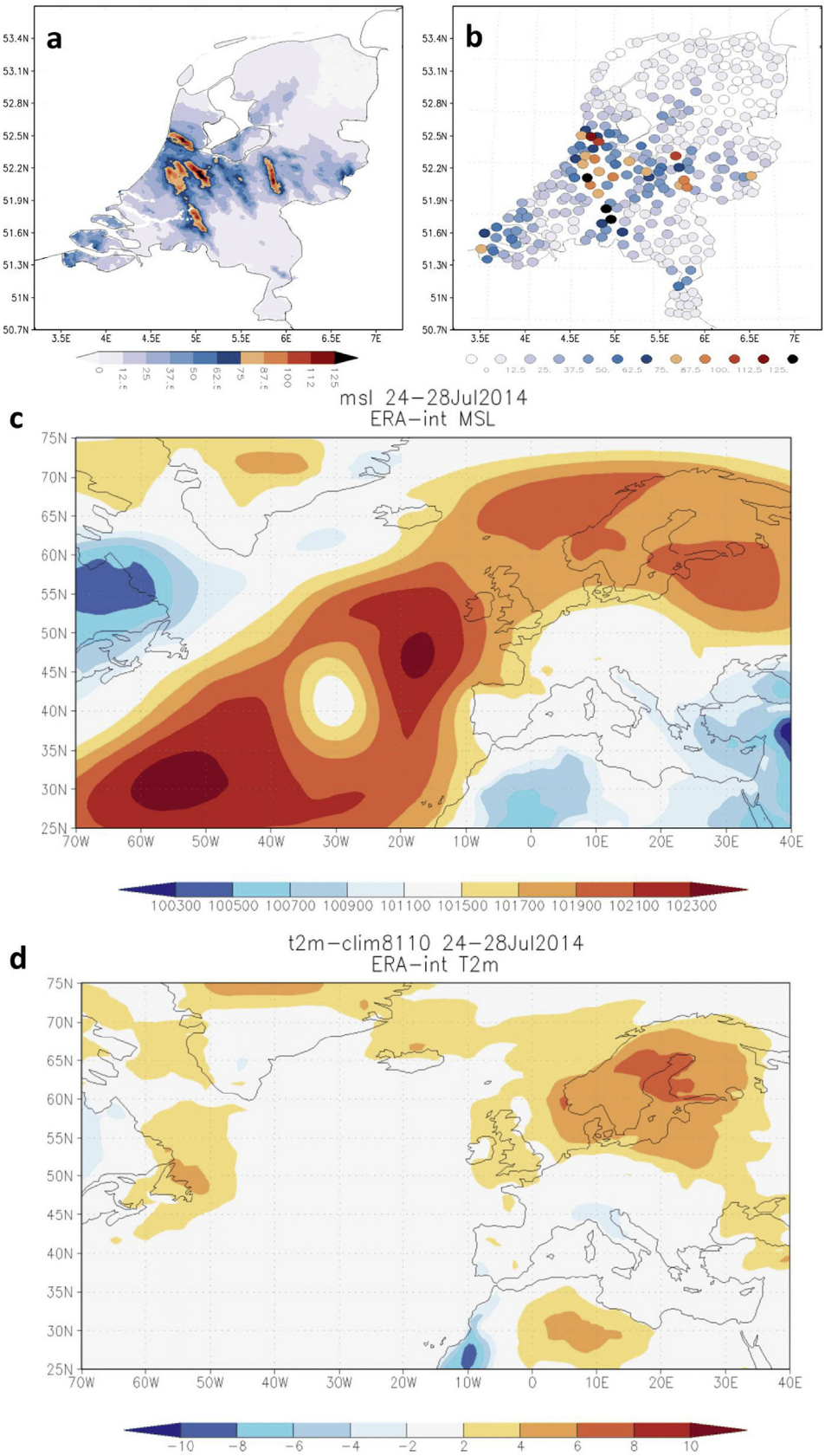

Fig. 1. (a) KNMI radar-derived precipitation on 28 July 2014 (0–24 UTC) b) 8-8 UTC station observations on 28 and 29 July, almost all of this is due to the event on the morning of 28 July. (c) Mean sea-level pressure (Pa) and (d) 2 m temperature anomalies (°C) with respect to 1981–2010, for 24–28 July 2014 from ERA-interim.

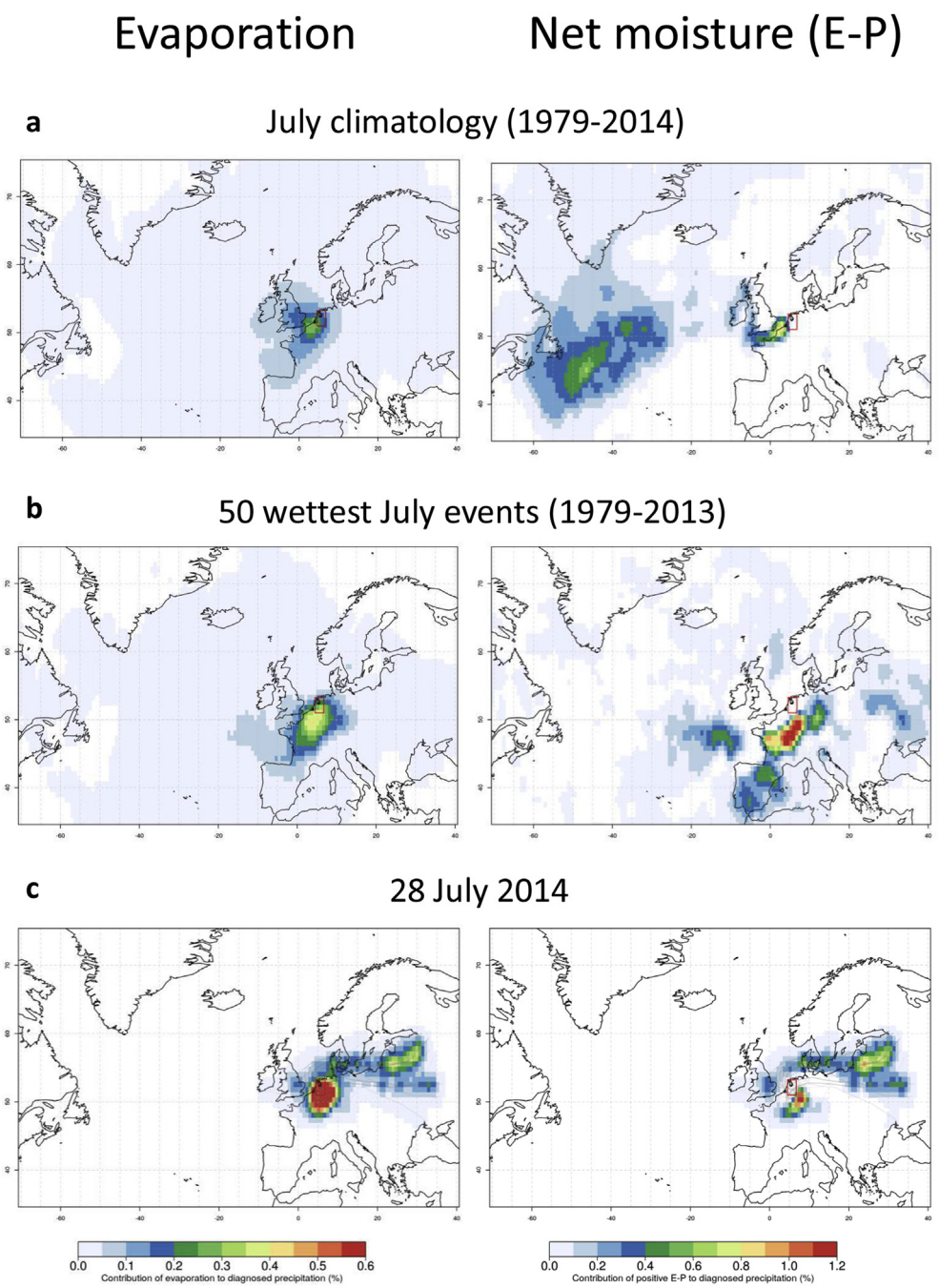

Fig. 2. Back trajectory derived cumulative contribution of evaporation (E; left panels) and evaporation minus precipitation (E-P; right panels) along diagnosed back trajectories to Netherlands for (a) all July days between 1979 and 2014, (b) the 50 wettest july days between 1979 and 2013 and (c) 28 July 2014, for which trajectories are overlain.

for the 50 wettest July precipitation events suggests that key regions of moisture gain for heavy daily precipitation events occur in continental Europe with the North Atlantic and other maritime sources less important to the overall moisture contribution (Fig. 2b). Analysis of the 28 July 2014 event itself shows two key source regions, both with similar net moisture contributions to precipitation during the event (Fig. 2c). The first appears to the south and southeast in southern Belgium and parts of western Germany. Given the relative proximity of this source to the target region it is difficult to offer a precise explanation of the transport of moisture. The second source of moisture is in the Baltic states and the moisture moved in a westerly direction across the Baltic and North Seas, accumulating more moisture, before sweeping southwards towards the Netherlands. With reference to Fig. 1, the second source is the combination of two synoptic-scale phenomena that contributed a substantial proportion of the accumulated moisture that fed the thunderstorms of 28 July 2014: (a) the anomalous high temperatures leading to enhanced evaporation in the Baltic region; and (b) an area of high pressure over Scandinavia driving a steady flow of moisture-laden air westwards. The sources and transport of moisture associated with this event were therefore not typical for convective high-precipitation episodes during summer.

In addition to the trajectory analysis, we also examined output of the regional climate model KNMI-RACMO (12 km resolution, downscaled from ERA-interim) to gain further insight into the origin of the convective instability and moisture transport (not shown). The simulations revealed a convergence line, extending from central France to

the Netherlands and a local increase in water vapour path (WVP). Convective showers developed at a few locations along the convergence line. Where showers occurred, the latent heat release led to very strong local increase in vertical velocity, almost one order of magnitude larger than the large scale vertical velocity associated with the frontal zone, and this brought in further moisture from the surroundings. In this case, it is thus not only the large-scale moisture transport which is of importance, but also the local thermodynamical feedback.

3. Event definition

A topic of several recent studies and opinion pieces is the implication of the so-called framing of the attribution question (Trenberth et al., 2015; Otto et al., 2016; Shepherd, 2016; National Academies of Sciences, Engineering, and Medicine, 2016). Each study, and its chosen methodology, poses an individual question at its outset concerning either a particular event (which will never occur in the same way again) or a 'class' of similar events. A number of different studies on the same event may therefore have different outcomes on the change in risk in response to climate change. Every individual extreme event is unique in terms of the external and internal processes that dictate its meteorological anatomy and it has been established in Section 2 that the processes involved in the development of the extreme precipitation event of 28 July 2014 were indeed rare. However, defining an event in terms of, say, a synoptic situation may be troublesome. Instead, an event definition that most directly relates to the risk, and therefore the impacts, of the event is more transparent and often more relevant to users. In the case of extreme precipitation and subsequent flooding, that risk-based definition is the class of events of actual precipitation amounts at or above a given threshold falling within a particular region over a given time period.

In our attribution analysis, we pose the question, "Has the likelihood of a 2014-type event changed as a result of anthropogenic climate change?". While it is crucial to ensure that the framing of the attribution question is communicated to and understood by the stakeholder, it is of equal importance to make clear the definition of the actual event being analysed (Otto et al., 2016). Here, the '2014-type' event is defined as a Netherlands-wide maximum one-day precipitation total of at least 131.6 mm occurring between April and September during a particular year. This definition is made with the following justifications.

(a) While the impacts of the 28 July 2014 event were due to sub-daily extremes of a few hours, the lack of hourly observational data in comparison to the dense station network recording daily precipitation totals coupled with the poor reliability of sub-daily precipitation processes in climate models makes such analysis impractical. We thus consider only 24-h precipitation totals and use the maximum observed value of 131.6 mm at an 0–24 station in our event definition.
(b) In considering the summer half year April–September only, we restrict our event definition to convective events. The large-scale precipitation extremes in the winter half year have different physical and statistical properties.
(c) In terms of spatial extent, our event classification considers only April–September one day precipitation maxima within the Netherlands. Again, this definition is largely driven by data availability, with a homogeneous countrywide set of station observations publicly accessible. Although the impacts of the 28 July 2014 were also felt outside of the Netherlands, the use of a clearly understood political boundary to define the event definition in geographical terms is beneficial when communicating to stakeholders.

4. Event exceptionality and trend detection

The primary basis for trend detection and establishing the role of anthropogenic climate change is the analysis of precipitation maxima within the observational record and climate model simulations using extreme value theory. The Generalised Extreme Value (GEV) distribution fitted to block maxima is a common approach to statistically model the distribution of precipitation extremes (Coles et al., 2001):

$$F(x) = exp\left[-\left(1+\xi\frac{x-\mu}{\sigma}\right)^{\frac{-1}{\xi}}\right] \quad (1)$$

where μ, σ and ξ are the location, scale and shape parameters of the distribution respectively. For ξ = 0 this reduces to the Gumbel distribution,

$$F(x) = exp\left[-exp\left(-\frac{x-\mu}{\sigma}\right)\right] \quad (2)$$

When it is anticipated that there is a dependence of the distribution of extremes on an external process, it is necessary for such a dependency to be reflected in the distribution parameters. Here, in order to assess the change in likelihood in precipitation extremes as a result of anthropogenic climate change, the GEV fit is assumed to scale linearly with an index representing global warming. This is taken as the global mean surface temperature smoothed with a four-year running mean in order to dampen the influence of interannual variability within the climate system, particularly ENSO. All data are fitted to a non-stationary GEV distribution, under the assumption that the dispersion parameter σ/μ and the shape parameter ξ do not vary (this assumption is checked in higher-statistics model data). The location parameter μ and hence scale parameter σ are assumed to vary with an exponential dependence on temperature to reflect the CC relation:

$$\mu = \mu_0 \cdot exp\frac{\alpha T}{\mu_0} \quad (3)$$

$$\sigma = \sigma_0 \cdot exp\frac{\alpha T}{\mu_0} \quad (4)$$

where μ_0 and σ_0 are the fit parameters of the distribution and α is the trend in precipitation maxima as a function of smoothed global mean surface temperature (GMST) anomaly T. The uncertainty margins were estimated using non-parametric bootstrapping with 1000 replications. The GEV scaling and non-parametric bootstrapping methods have been applied previously to event attribution analysis (e.g., Schaller et al., 2014; Eden et al., 2016; Otto et al., 2018).

We first of all use Eq. (1) to fit observations at many stations simultaneously. This usually assumes that precipitation at these stations is independent and identically distributed. The second clause, identical distributions, holds well in the Netherlands. The orography is not pronounced and coastal effects do not play a large role as the most intense systems usually come from land, from France through Belgium or, rarely, Germany. Urban effects have been shown to be small (Daniels et al., 2016). However, observations at these stations, about 10 km apart, are not independent, not even for the summer maximum of one-day precipitation. Spatial dependencies between the stations were taken into account using a moving block technique. Cross correlation is performed on the time series of precipitation maxima at all stations; each bootstrap sample includes a station chosen at random and other stations that are positively correlated ($r > 1/e$) with that station. Serial autocorrelations could be treated similarly, but are negligible here. The fit routine is available via the KNMI Climate Explorer (http://climexp.knmi.nl).

The GMST-dependent GEV methodology was applied to station data in order to quantify the exceptionality of the 28 July 2014 event in the observational record and the change in its likelihood over the last century. First of all, a GEV was fitted to annual maxima in April–September daily precipitation at the 102 homogenised volunteer stations for 1910–2016, excluding the year of the extreme event in question, 2014. The maximum observed precipitation value for 28 July

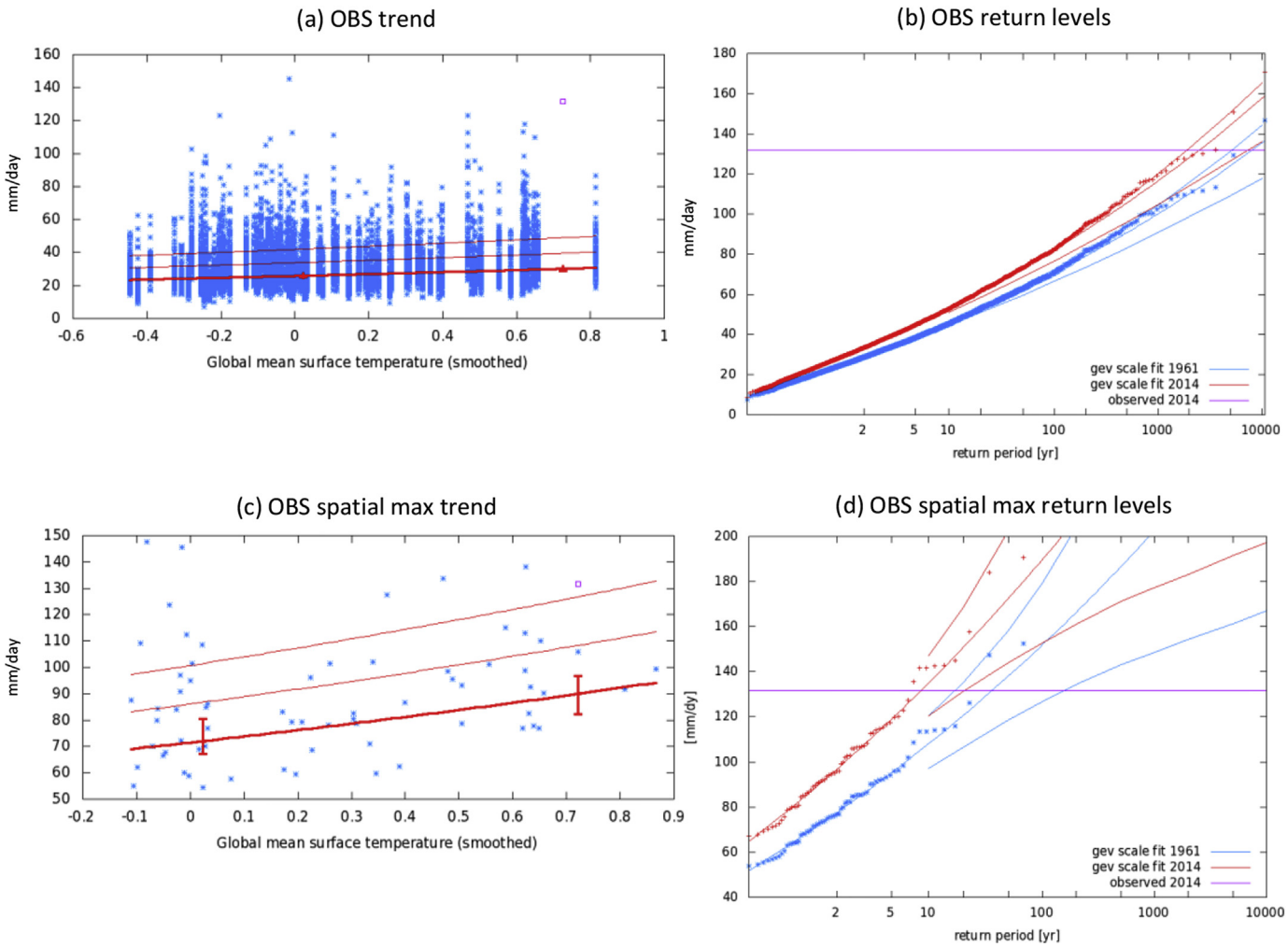

Fig. 3. (a) Relationship between observed annual maxima in April–September daily precipitation totals and global mean surface temperature (GMST) for 1910–2016. Shown are the location parameter μ (thick line), $\mu+\sigma$ and $\mu+2\sigma$ (thin lines). The 28 July 2014 event is denoted by the purple square. (b) Gumbel plot showing the non-stationary GEV fit scaled to the smoothed GMST of 2014 (central red line; bounding red lines represent 95% confidence intervals) and 1961 (blue). The observations are drawn twice, scaled up to 2014 (red markers) and 1961 (blue markers) using the fitted trend. The 28 July 2014 event is denoted by the purple line. (c–d) As (a) and (b) but for GEV fitted to spatial (Netherlands-wide) maxima. (For interpretation of the references to colour in this figure legend, the reader is referred to the Web version of this article.)

2014 among this data is 107.7 mm. However, as these stations record only data between 8 and 8 UTC, a sizeable fraction of the precipitation that fell during the morning is recorded on 29 July 2014. The 28 July 2014 maximum observed value is therefore still considered to be the 131.6 mm total recorded at the 0–24 UTC automatic weather station at Deelen.

A positive trend is found in precipitation maxima in all observational data (significant at the 95% level) (Fig. 3). When fitted to the 102 homogenised stations and scaled to the climate of 1961, a 2014-type event has a return period of approximately 8000 years (Fig. 3a). In the climate of 2014 the return period has reduced to approximately 3000 years. The change in probability of an event of the magnitude of 2014 due to climate change may be quantified by the probability (or risk) ratio (PR) defined as PR = P_1/P_0 where P_1 is the probability of exceeding a specified threshold in the current climate and P_0 is the probability of exceeding the same threshold is some past climate (e.g. Fischer and Knutti, 2015; Stott et al., 2016). For a one-day precipitation total of 131.6 mm, a probability ratio of roughly 3.1 was found, within a 95% confidence interval (CI) range of 2.4–3.6, showing an increase in the likelihood of a 2014-type event between 1961 and 2014 as a result of an increase in global mean temperature.

The return periods calculated are for this amount of precipitation falling at a predetermined location and therefore correspond closely to design criteria, which typically are 1 in 100 years or less for local precipitation: e.g., 1 in 100 years for low-lying polders, 1 in 250 years for flooding of motorways. These values were exceeded at many places on 28 July 2014.

We also consider high-intensity events that occur *somewhere* in the Netherlands. A GEV fit to annual *spatial* (Netherlands-wide) maxima in April–September one-day precipitation (i.e. occurring at any station) gives a return period of only 10 years (CI range 6–24 years) in the climate of 2014 (Fig. 3c–d). In spite of the highest two values being in 1951 (Amsterdam) and 1975 (Gouda) the trend is significantly positive, with a probability ratio for the climate of 2014 relative to 1961 of 3.2 (CI range 1.2–16). This is compatible with the trends obtained from all stations simultaneously but with a larger uncertainty, as it uses only a high-intensity subset of the events.

5. Models and evaluation

The statistical methodology detailed in Section 4 was subsequently applied to the output of a number of global (GCMs) and regional climate models (RCMs) varying in resolution and setup. It is important to consider the difference between observed precipitation at the point

Table 1
Details for the GCM and RCM ensembles considered in the attribution analysis. The 7 models included in the CORDEX sub-ensemble are also detailed.

GCMs		Resolution	Analysis period	Ensemble size
EC-EARTH2.3		1.125° × 1.125°	1860–2100	16
HadGEM3-A		0.833° × 0.555°	1960–2013	15
RCMs	**Driving GCM**	**Resolution**	**Analysis period**	**Ensemble size**
RACMO	EC-EARTH2.3	0.11° × 0.11°	1961–2015	16
CORDEX subset	Various	0.11° × 0.11°	1971–2015	7
CORDEX models	**Driving GCM**	**Resolution**	**Analysis period**	**Ensemble size**
CCLM4-8-17	CNRM-CM5	0.11° × 0.11°	1950–2015	1
HIRHAM5	EC-EARTH2.3	0.11° × 0.11°	1950–2015	1
RACMO22E	EC-EARTH2.3	0.11° × 0.11°	1950–2015	1
RCA4	EC-EARTH2.3	0.11° × 0.11°	1969–2015	1
RCA4	HadGEM2-ES	0.11° × 0.11°	1969–2015	1
REMO2009	MPI-ESM-LR	0.11° × 0.11°	1950–2015	2
WRF331F	IPSL-CM5A-MR	0.11° × 0.11°	1951–2015	1

scale and the area-averaged precipitation represented by model output. Clearly the degree to which a model is able to reproduce real world precipitation totals is dependent on its resolution as well as its internal physics and parameterisation. Whilst we conduct and emphasise the importance of an initial validation of model precipitation characteristics, which in this case considers the distribution of daily extremes and then areal scaling, it is still necessary to communicate caveats. The extent to which models are able to reproduce observed trends at small scales has been the subject of recent debate (e.g. Maraun, 2016). In particular, convection-permitting or -resolving models may be necessary to describe these events well.

Details of all models used are given in Table 1. Firstly two GCMs were considered: EC-Earth 2.3 (coupled) and HadGEM3-A (SST-forced). For EC-Earth 2.3, analysis was applied to a 16-member ensemble at T159L62 (approximately 1.125° × 1.125°) resolution for the period 1860–2015 (Hazeleger et al., 2010), following the CMIP5 framework (Taylor et al., 2012) with historical conditions 1860–2005 and RCP8.5 for 2006–2015. For HadGEM3-A, analysis was undertaken for two 15-member ensembles at a N216 (approximately 0.833° × 0.555°) resolution for the period 1960–2013 (Christidis et al., 2013). The first was driven with observed forcings (including anthropogenic forcings) and sea-surface temperatures (hereafter 'historical' or ANT). The second was a 'counterfactual' ensemble driven with pre-industrial forcings and sea-surface temperatures adjusted downward by a climate change pattern obtained from the CMIP5 ensemble ('historicalNat' or NAT), and thus representative of the evolution of a climate system in a world without anthropogenic climate drivers. As all ensemble members were driven by the same SST the data are not independent. This is accounted for in the same way as the spatial dependencies were in the observational analysis.

In section 2, we identified the synoptic situation during the 28 July 2014 event that contributed to the event's exceptionality. While not necessary conditions for a 2014-type event according to our definition, the features characterised by a north-south pressure dipole and anomalous temperature over Scandinavia highlight the importance of atmospheric circulation in transporting the moisture quantities that contribute to extreme precipitation events. It is therefore reasonable to assess the pair of GCM ensembles on their representation of the background synoptic fields and their variability. Both EC-Earth 2.3 and HadGEM3-A are able to reproduce realistic means in near surface temperature and sea level pressure between April and September (Fig. 4). EC-Earth 2.3 marginally underestimates the variance in April to September temperature across Central and Eastern Europe but we are still able to assume that each ensemble has the capacity to simulate the breadth of synoptic conditions that potentially lead to episodes of extreme precipitation within the Netherlands.

The same statistical methodology used to conduct attribution analysis of model output was extended to higher resolution RCMs. First of all, KNMI-RACMO (Meijgaard et al., 2008, 2012) was used to downscale each of the 16 EC-Earth 2.3 ensemble members over Western Europe for the period 1950–2100 at a resolution of 0.11°, which is still not convection-permitting. Secondly, output was taken from the EURO-CORDEX project, a coordinated set of high-resolution (approximately 12 km × 12 km) climate projections for Europe and the North Atlantic. Data was taken from fourteen experiments using historical forcings up to 2005 and the RCP8.5 scenario for the period 2006–2015. With the exception of the REMO2009 experiment driven by MPI-ESM-LR, which features two initialisations, all experiments feature only one ensemble member thereby reducing the number of annual maxima for GEV fitting. To counter this, a sub-ensemble was generated from a subset of seven bias-adjusted EURO-CORDEX (Jacob et al., 2014). Bias adjustment is undertaken using the WFDEI data set (Weedon et al., 2011) with a Cumulative Distribution Function transform (CDFt) (Vrac et al., 2012) used to preserve trends in the adjustment. Details of the models used in the sub-ensemble subset are given in Table 1. It is important to note that not all members within the sub-ensemble are independent due to experiments involving the same RCM or driving GCM. However, the same bootstrapping technique that deals with spatial dependencies between neighbouring grid points is also able to take into account any inter-member dependencies.

Models have difficulty in reproducing daily precipitation totals similar in magnitude to the 28 July 2014 event and statistical correction is necessary to account for model biases. Such biases are in part due to the difference in areal representation of point-scale observations and grid-based model output. A simple multiplicative scaling, based the ratio of the scale parameters of the stationary GEV fitted to station and modelled maxima respectively ($\sigma_{obs}/\sigma_{mod}$), is used as a first order correction for model bias. In dealing with extremes, in this case block maxima, assessment of the scope for the application of the multiplicative scaling requires comparison of the GEV distribution fitted to model output with that fitted to observations. To allow for the possibility of a correction, we demand that the GEV parameters of a fit to model output are plausible by comparing the ratio of the scale and location parameters, σ/μ. The HadGEM3-A, RACMO and EURO-CORDEX ensembles all produce σ/μ ratios within the range 0.25–0.32. This is broadly consistent with the σ/μ ratio when fitted to observed maxima (0.31) (note that to ensure the fit to observed data is made with a number of data points similar in magnitude to that used in the fitting

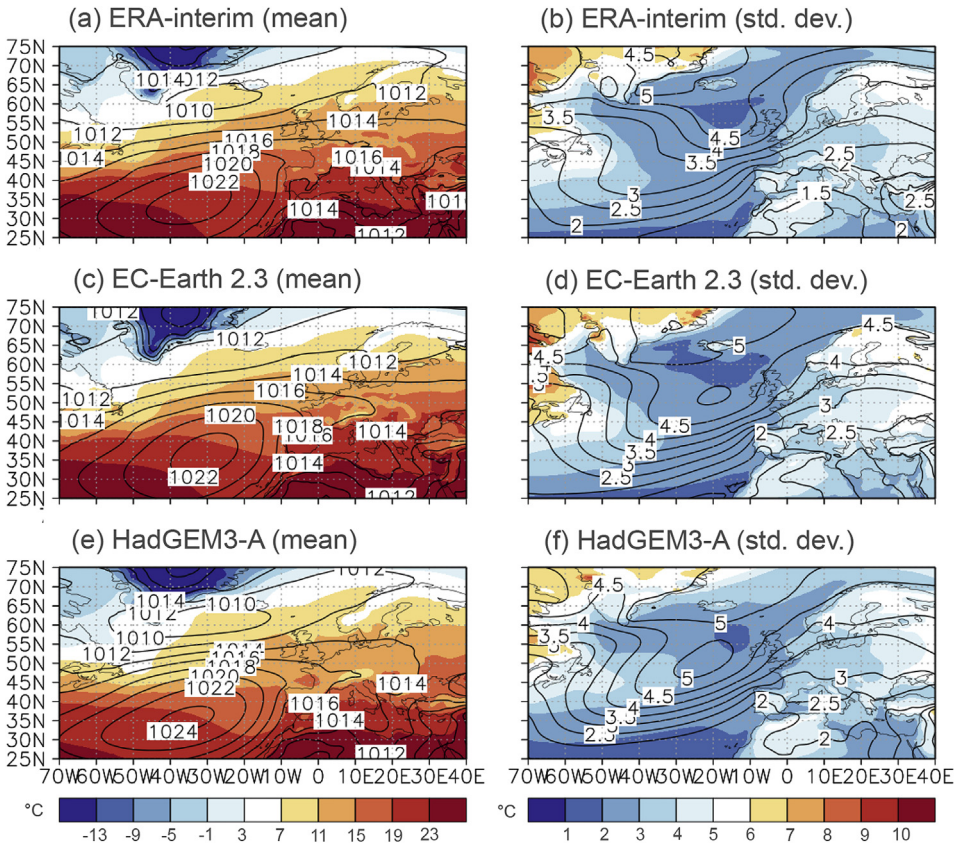

Fig. 4. Mean (left panels) and standard deviation (right panels) statistics for April to September near surface temperature (shaded contours) and mean sea level pressure (solid contours) for (a) ERA-interim and the (b) EC-EARTH2.3 and (c) HadGEM3-A ensembles (1979–2014).

for the model ensembles, the GEV is fitted with data from all observation points rather than spatial maxima). For EC-Earth 2.3, the ratio σ/μ was far smaller (0.18). It was concluded that, as the dispersion of the GEV fitted to EC-Earth 2.3 output was not in agreement with that fitted to observations, any model bias in precipitation maxima could not be corrected using a simple multiplicative correction. The contribution of EC-Earth 2.3 to further analysis was therefore rejected.

The area-averaged model output has far larger decorrelation scales than the observations, showing only one or two degrees of freedom in the Netherlands rather than the 30 of the station data. This implies that the grid points are too dependent to reliably fit a GEV to. We therefore only considered the spatial maximum of the April–September maximum of daily precipitation.

6. Attribution analysis

The GMST-dependent GEV approach described in Section 4 was applied to Netherlands-wide annual maxima of April–September one-day precipitation totals from the GCM and RCM ensembles. As with the GEV fit made to observations, the 2014 April–September maximum is excluded. Fig. 5 shows the relationship between GMST and precipitation maxima in the ensembles (left panels) and the GEV fits for the precipitation maxima from each ensemble (right panels). The data from all three models is described well by the GEV distribution with some exception for the very highest extremes, which is to be expected (van den Brink and Können, 2008). For the historically-forced (ANT) HadGEM3-A ensemble, a significant positive trend is found in precipitation maxima ($p < 0.05$) (Fig. 5a–b). No trend is found in the naturally-forced (NAT) ensemble (Fig. 5c–d). There is no significant trend found in either RACMO (Fig. 5e–f) or the CORDEX sub-ensemble (Fig. 5g–h).

In order to make an attribution statement that is specific to a 2014-type event according to our definition, multiplicative scaling based on the ratio of the scale parameters of the stationary GEV fitted to station and modelled maxima respectively ($\sigma_{obs}/\sigma_{mod}$) was used to account for model bias. It was assumed that the $\sigma_{obs}/\sigma_{mod}$ ratio is applicable to spatial maxima. For each model ensemble, the correction is applied in order to scale the 28 July 2014 event maximum of 131.6 mm to an equivalent magnitude in the model distribution, so the grid box probability density function was used to approximate the station observations. These 2014-equivalent magnitudes, which are indicated by the solid horizontal lines in Fig. 5 (right panels), were subsequently used to calculate probability ratios. For the historically-forced HadGEM3-A ensemble, the likelihood of a 2014-type event was found to have changed by a factor of 1.5 within the 95% CI range 1.0–1.9 between 1961 and 2014. Equivalently, we can say there is an expected change of 8% (−1%–11%) in the magnitude of an event of the observed return period, between 1961 and 2014. For the RACMO ensemble, a 2014-type event was found to be between 0.4 and 1.5 times more likely in 2014 than in 1961, with a change in magnitude of between −4% and 5%. For the CORDEX sub-ensemble, while no significant trend was found in Fig. 5g, there is a larger tendency in the bootstrap towards a decrease in likelihood than an increase with a probability ratio of between 0.4 and 1.5, and a change in magnitude of between −18% and 7%.

The different setups of the historically and naturally forced HadGEM3-A ensembles provides a basis for the influence of anthropogenic emissions explicitly. In this case the probability ratio was calculated by comparing the return periods scaled to the climate of 2014 in the ANT and NAT ensembles and therefore representative of the change in likelihood solely as a result of anthropogenic forcing. As the ANT and NAT ensembles originate from the same model, the same multiplicative scaling is applied to each. For a 2014-type event, a ratio of 1.2 was found within a 95% CI range of 0.4–3.2. Unlike in the comparison of the GEV fit scaled to different GMST in the single scenario, the percentage

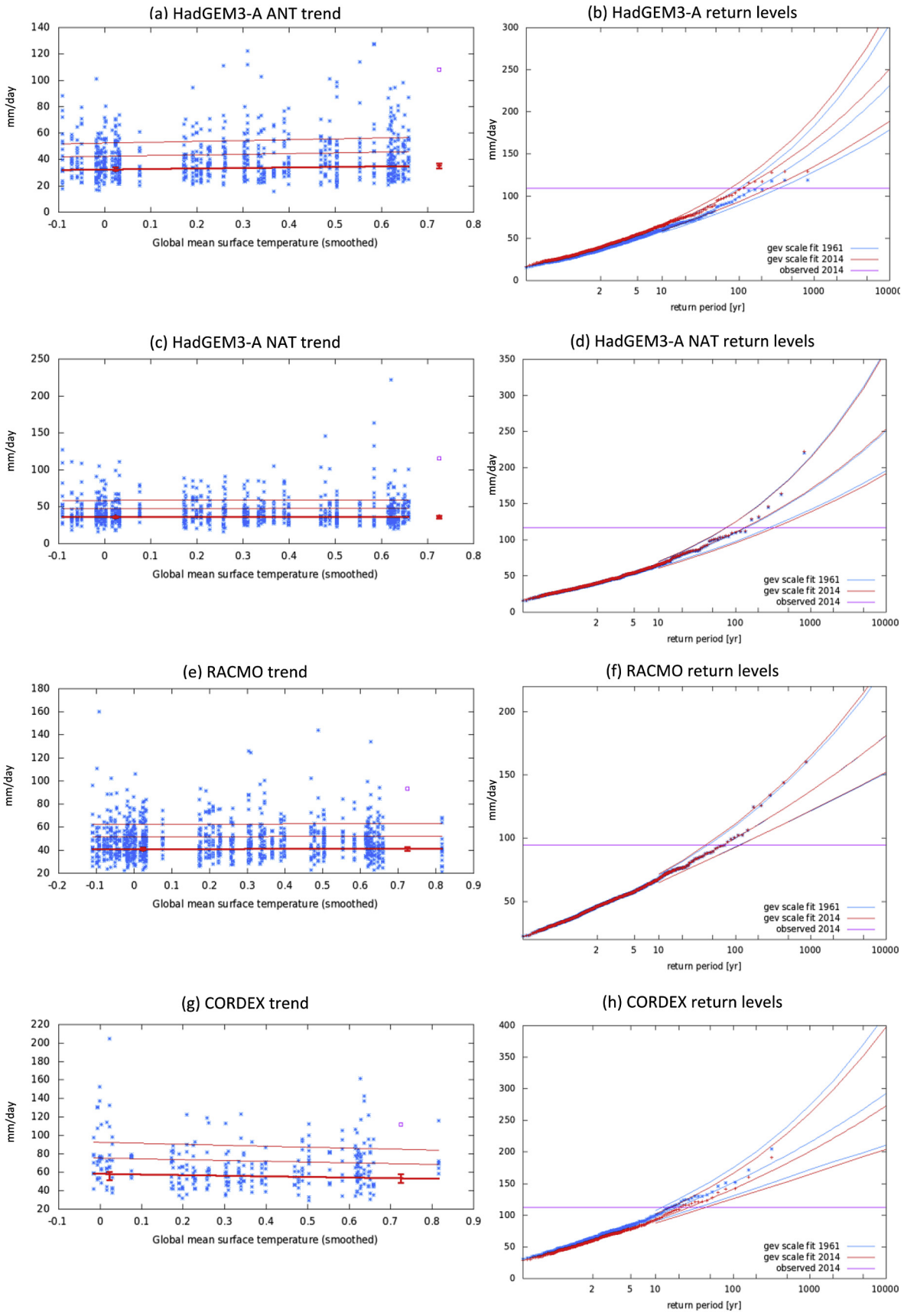

(caption on next page)

Fig. 5. (a) Relationship between annual maxima in April–September daily precipitation totals from HadGEM3-A (ANT) and observed GMST. Shown are the location parameter μ (thick line), $\mu+\sigma$ and $\mu+2\sigma$ (thin lines). The 28 July 2014 event scaled to the model distribution is denoted by the purple square. (b) Gumbel plot showing the non-stationary GEV scaled to the smoothed GMST of 2014 (central red line; bounding red lines represent 95% confidence intervals) and 1961 (blue). The observations are drawn twice, scaled 2014 (red markers) and 1961 (blue markers) using the fitted trend. The 28 July 2014 event, scaled to the model distribution using bias correction, is denoted by the purple line. (c–d) As (a) and (b) but for the HadGEM3-A (NAT) ensemble. (e–f) As (a) and (b) but for the RACMO ensemble. (g–h) As (a) and (b) but for the EURO-CORDEX ensemble. (For interpretation of the references to colour in this figure legend, the reader is referred to the Web version of this article.)

change in precipitation magnitude is not independent of the return time for which it is evaluated. The ANT-NAT differences in magnitude were therefore evaluated for precipitation events with a 100-year return time in order to produce uncertainty estimates that are comparable with the previous observation- and model-based analysis. The change in magnitude of 4% was found within a 95% CI range of −15% to 20%. The two different analyses of HadGEM3-A allow for a check on the assumption of constant σ/μ and ξ. Indeed, the fit of the historical experiment to a GEV dependent on smoothed GMST and the fit of the histroicalNat counterfactual world to a constant GEV fit give the same dispersion and shape parameters, confirming the assumptions of Eqs. (3) and (4) in this model.

A summary of the probability ratios calculated for the both the observation- and model-based methods are shown in Fig. 6a. The difference in likelihood is given with respect to the change in global mean surface temperature between the pre-industrial era and (approximately) the present day, as represented by the inter-scenario probability ratio derived between the ANT and NAT HadGEM3-A ensembles. In the other methods the probability ratios are derived for the period between 1961 and 2014 and are thus only partially representative of the change since pre-industrial conditions. All probability ratios initially calculated for 1961 to 2014 are raised to the power of 1.25 in order to represent the influence of anthropogenic climate change from the pre-industrial era to 2014. Likewise, the percentage changes derived for 1961 to 2014 are multiplied by 1.25 (Fig. 6b).

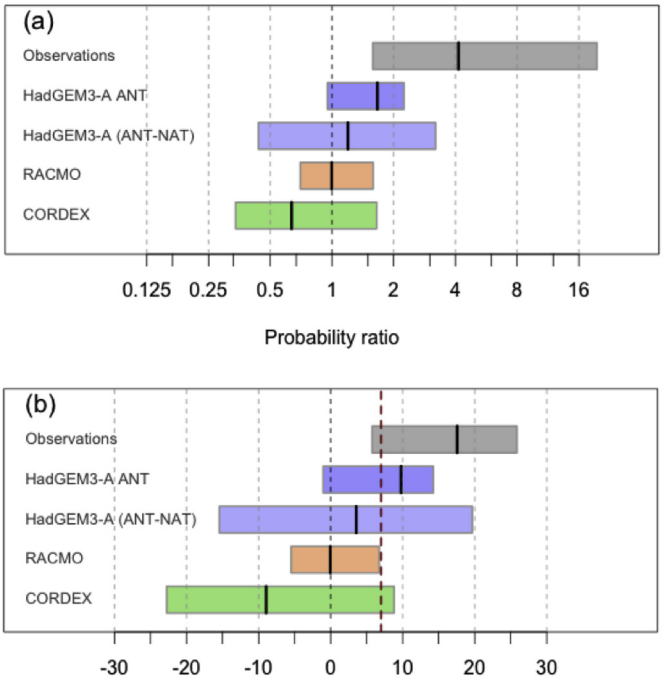

Fig. 6. (a) Summary of the probability ratios for a 2014-type event derived from analysis of observed and simulated spatial maxima. (b) Summary of percentage change in the magnitude of daily precipitation spatial maxima derived from different methods. The red dashed line indicates the expected change in magnitude according to the Clausius-Clapeyron relation. Bars in both (a) and (b) are representative of the 95% confidence intervals. For observations, results are based on analysis of the spatial maxima of 102 homogenised stations. All results represent change between the pre-industrial era and 2014. (For interpretation of the references to colour in this figure legend, the reader is referred to the Web version of this article.)

The spread of the observation- and model-based results is somewhat larger than expected by natural variability alone, with $\chi^2/\text{dof} \approx 2.8$. If we accept that the spread is just due to random weather variability it is possible to interpret the results collectively, either by taking a multi-method average or weighting each result by its uncertainty. Aside from the CORDEX sub-ensemble, the central values of each method are consistent with a positive change in the likelihood of extremes. The CORDEX sub-ensemble uses single realisations of different models rather than multiple realisations of one model and hence is bias corrected for each model separately. The degree to which the resulting uncertainty influences the representation of the trend in this ensemble is beyond the scope of this study. The higher trend in the observations can under these assumptions be only partially attributed to global warming with the observed increase largely due to natural variability.

However, taking into account the underlying physics and results from other work, there is another interpretation of the results. The models considered have resolutions that do not resolve convection and rely on parameterisations of these processes on the sub-grid scale. The trends at both global and local scales from these types of models are often seen to be smaller than the trends in observations (e.g., Min et al., 2011; Eden et al., 2016). If this is indeed a systematic deficiency of the models considered, the best interpretation could be that the observed trend is due to global warming and the modelled trends are too small. Convection-permitting models are necessary if this possibility is to be fully investigated.

7. Discussion and conclusions

Establishing the role of anthropogenic climate change on the likelihood of small-scale, short-term episodes of extreme precipitation poses a number of challenges within the emerging field of attribution science (National Academies of Sciences, Engineering, and Medicine, 2016). Here, a probabilistic event attribution case study has been undertaken on the extreme precipitation event that occurred in the Netherlands on 28 July 2014. An established method based on extreme value distributions fitted to precipitation maxima in observed and model-simulated data has been used to produce a clear attribution statement.

An initial analysis of the large-scale circulation associated with the 28 July 2014 event, including diagnosis of moisture sources and transport, demonstrated the exceptionality of the event in synoptic terms. However, our event definition focused on the daily precipitation total, irrespective of the meteorological processes that led to it. This definition is more relevant to end users requiring information about how often a precipitation event of a particular magnitude, rather than a similar synoptic situation, might occur. In our final conclusions and attribution statements, we consider the change in likelihood of a 2014-type event, which was defined as an annual Netherlands-wide maximum in one-day precipitation occurring during April–September in excess of 131.6 mm. A GEV distribution assumed to scale with smoothed global mean surface temperature, fitted with annual Netherlands-wide one-day April–September precipitation maxima at 102 observation stations for the period 1910–2016, allowed us to conclude that the return period for a 2014-type event occurring at any

of these stations is around 10 years (CI range 6–24 years). The second analysis was extended to a number of global and regional model ensembles, chosen following an evaluation of the potential for the systematic bias in each to be corrected using multiplicative scaling. These models range in resolution from 60 km to 11 km. None of them are convection-permitting, so that the events being simulated are not directly resolved but depend on parameterisations.

The results are not unequivocal. Based on the best estimates from observations alone, we can conclude that there is a strong increase in intensity (around 18% within a CI range of 6%–26%) and frequency (by a factor of 4 within a CI range of 2–19) of 2014-type events since the pre-industrial era but the trends in the three model ensembles are somewhat smaller. In the context of how the attribution question is framed, it is important to note that the different model ensembles address slightly different questions given the differences in boundary conditions and resolution. While it is not possible to interpret the attribution results in relation to the different constraints on the model experiments, all model-based results (with the exception of EC-Earth 2.3) constitute a valid approach to event attribution and are therefore complementary in addressing to what extent anthropogenic climate change has changed the likelihood of a 2014-type event.

Consistent with the considerable natural variability, we offer two possible interpretations in the synthesis of our observation- and model-based results. The first interpretation is that the differences between the trends in observations and the three model ensembles considered are due to different noise realisations. The higher trend in the observations is then interpreted as due to chance fluctuations. The second interpretation is based on the fact that none of the three model ensembles is convection-permitting and therefore at risk of underestimating the trend. Unfortunately, the long runs or large ensembles required for event attribution are not yet available for convection-permitting models. If we assume that the models that parameterise convection underestimate the trend, our conclusion is limited to the trend found in the observations.

To summarise, the observations show a strong increase in the likelihood of local precipitation extremes similar to the event observed on 28 July 2014, albeit with large uncertainty margins due to natural variability. With the addition of information from climate models, it was shown that a fraction of change can be attributed to global warming. The remainder is due either to natural variability or to an underestimation of the trend in models. In our introduction, we noted the challenges in attributing extreme precipitation events, particularly small-scale events associated with convective activity. Our results are associated with considerable uncertainty and highlight the difficulty in conducting attribution analysis on events of this nature. Application of our methods to convection-permitting model ensembles that are able to better reproduce the observed trend will likely yield a more robust attribution statement.

Acknowledgements

We acknowledge the E-OBS dataset from the EU-FP6 project ENSEMBLES (http://ensembles-eu.metoffice.com) and KNMI (data downloaded via ECA&D, http://www.ecad.eu). This project was supported by the EU project EUCLEIA under Grant Agreement 607085.

References

Berg, P., Haerter, J., Thejll, P., Piani, C., Hagemann, S., Christensen, J., 2009. Seasonal characteristics of the relationship between daily precipitation intensity and surface temperature. J. Geophys. Res.: Atmosphere 114 (D18).

Buishand, T.A., De Martino, G., Spreeuw, J.N., Brandsma, T., 2013. Homogeneity of precipitation series in The Netherlands and their trends in the past century. Int. J. Climatol. 33, 815–833.

Christidis, N., Stott, P.A., Scaife, A.A., Arribas, A., Jones, G.S., Copsey, D., Knight, J.R., Tennant, W.J., 2013. A new HadGEM3-A-based system for attribution of weather- and climate-related extreme events. J. Clim. 26, 2756–2783.

Coles, S., Bawa, J., Trenner, L., Dorazio, P., 2001. An Introduction to Statistical Modeling of Extreme Values 208 Springer.

Daniels, E.E., Lenderink, G., Hutjes, R.W.A., Holtslag, A.A.M., 2016. Observed urban effects on precipitation along the Dutch West coast. Int. J. Climatol. 36, 2111–2119. https://doi.org/10.1002/joc.4458.

Dee, D., Uppala, S., Simmons, A., Berrisford, P., Poli, P., Kobayashi, S., Andrae, U., Balmaseda, M., Balsamo, G., Bauer, P., et al., 2011. The ERA-Interim reanalysis: configuration and performance of the data assimilation system. Q. J. R. Meteorol. Soc. 137 (656), 553–597.

Dominguez, F., Kumar, P., Liang, X.-Z., Ting, M., 2006. Impact of atmospheric moisture storage on precipitation recycling. J. Clim. 19 (8), 1513–1530.

Eden, J.M., Wolter, K., Otto, F.E.L., Oldenborgh, G.J. van, 2016. Multi-method attribution analysis of extreme precipitation in Boulder, Colorado. Environ. Res. Lett. 11, 124009.

Fischer, E.M., Knutti, R., 2015. Anthropogenic contribution to global occurrence of heavy-precipitation and high-temperature extremes. Nat. Clim. Change 5 (6), 560–564.

Hartmann, D.L., Klein Tank, A.M.G., Rusticucci, M., Alexander, L.V., Brnnimann, S., Charabi, Y., Dentener, F.J., Dlugokencky, E.J., Easterling, D.R., Kaplan, A., Soden, B.J., Thorne, P.W., Wild, M., Zhai, P.M., 2013. Observations: atmosphere and surface. In: climate change. In: Stocker, T.F., Qin, D., Plattner, G.-K., Tignor, M., Allen, S.K., Boschung, J., Nauels, A., Xia, Y., Bex, A., Midgley, P.M. (Eds.), The Physical Science Basis. Contribution of Working Group I to the Fifth Assessment Report of the Intergovernmental Panel on Climate Change. Cambridge University Press, Cambridge, United Kingdom and New York, NY, USA.

Hazeleger, W., Severijns, C., Semmler, T., Stefanescu, S., Yang, S., Wang, X., Wyser, K., Dutra, E., Baldasano, J.M., Bintanja, R., et al., 2010. EC-EARTH: a seamless earth-system prediction approach in action. Bull. Am. Meteorol. Soc. 91 (10), 1357–1363.

Hoerling, M., Wolter, K., Perlwitz, J., Quan, X., Eischeid, J., Wang, H., Schubert, S., Diaz, H., Dole, R., 2014. Northeast Colorado extreme rains interpreted in a climate change context. Bull. Am. Meteorol. Soc. 95 (9), S15–S18.

van den Hurk, B.J., van Meijgaard, E., 2010. Diagnosing land-atmosphere interaction from a regional climate model simulation over West Africa. J. Hydrometeorol. 11 (2), 467–481.

Jacob, D., et al., 2014. EURO-CORDEX: new high-resolution climate change projections for European impact research. Reg. Environ. Change 14 (2), 563–578.

Kay, A.L., Crooks, S.M., Pall, P., Stone, D.A., 2011. Attribution of Autumn/Winter 2000 flood risk in England to anthropogenic climate change: a catchment-based study. J. Hydrol. 406, 97–112.

Lenderink, G., Barbero, R., Loriaux, J.M., Fowler, H.J., 2017. Super Clausius-Clapeyron scaling of extreme hourly convective precipitation and its relation to large-scale atmospheric conditions. J. Clim.

Loriaux, J.M., Lenderink, G., Siebesma, A.P., 2016. Peak precipitation intensity in relation to atmospheric conditions and large-scale forcing at midlatitudes. J. Geophys. Res. Atmos. 1–17. https://doi.org/10.1002/2015JD024274. http://doi.wiley.com/10.1002/2015JD024274.

Maraun, D., 2016. Bias correcting climate change simulations - a critical review. Curr. Clim. Change Rep. 2, 211. https://doi.org/10.1007/s40641-016-0050-x.

Meijgaard, E. van, Ulft, L.H. van, Berg, W.J. van de, Bosveld, F.C., Hurk, B.J.J.M. van den, Lenderink, G., Siebesma, A.P., 2008. The KNMI Regional Atmospheric Climate Model RACMO Version 2.1, Tech. Rep. Koninklijk Nederlands Meteorologisch Instituut.

Meijgaard, E. van, Ulft, L.H. van, Lenderink, G., De Roode, S.R., Wipfler, E.L., Boers, R., Timmermans, R.M.A. van, 2012. Refinement and application of a regional atmospheric model for climate scenario calculations of Western Europe. Tech. Rep. KVR 054/12 (KVR).

Min, S.K., Zhang, X., Zwiers, F.W., Hegerl, G.C., 2011. Human contribution to more-intense precipitation extremes. Nature 470, 378–381.

National Academies of Sciences, Engineering, and Medicine, 2016. Attribution of Extreme Weather Events in the Context of Climate Change. The National Academies Press, Washington, DC. https://doi.org/10.17226/21852.

van den Brink, H.W., Können, G.P., 2008. The statistical distribution of meteorological outliers. Geophys. Res. Lett. 35 (23).

van Oldenborgh, G.J., Van Urk, A., Allen, M.R., 2012. The absence of a role of climate change in the 2011 Thailand floods. Bull. Am. Meteorol. Soc. 93 (7), 1047–1049.

Van Oldenborgh, G.J., Philip, S., Aalbers, E., Vautard, R., Otto, F.E.L., Haustein, K., Habets, F., Singh, R., Cullen, H., 2016. Rapid attribution of the May/June 2016 flood-inducing precipitation in France and Germany to climate change. Hydrol. Earth Syst. Sci. Discuss. https://doi.org/10.5194/hess-2016-308.

Otto, F.E.L., van Oldenborgh, G.J., Eden, J.M., Stott, P.A., Karoly, D.J., Allen, M.R., 2016. Framing the question of attribution of extreme weather events. Nat. Clim. Change 6, 813–816.

Otto, F.E.L., van der Wiel, K., van Oldenborgh, G.J., Philip, S., Kew, S.F., Uhe, P., Cullen, H., 2018. Climate change increases the probability of heavy rains in Northern England/Southern Scotland like those of storm Desmond – a real-time event attribution revisited. Environ. Res. Lett. 13, 024006.

Schaller, N., Otto, F.E.L., van Oldenborgh, G.J., Massey, N.R., Sparrow, S., Allen, M.R., 2014. The heavy precipitation event of May-June 2013 in the upper Danube and Elbe basins. Bull. Am. Meteorol. Soc. 95 (9), S69.

Shepherd, T.G., 2016. A common framework for approaches to extreme event attribution. Curr. Clim. Change Rep. 2 (1), 28–38.

Stott, P.A., Christidis, N., Otto, F.E., Sun, Y., Vanderlinden, J.P., van Oldenborgh, G.J., Vautard, R., von Storch, H., Walton, P., Yiou, P., Zwiers, F.W., 2016. Attribution of extreme weather and climate-related events. Wiley Interdisciplinary Reviews: Climate Change 7 (1), 23–41.

Taylor, K.E., Stouffer, R.J., Meehl, G.A., 2012. An overview of CMIP5 and the experiment design. Bull. Am. Meteorol. Soc. 93 (4), 485–498.

Trenberth, K.E., Fasullo, J.T., Shepherd, T.G., 2015. Attribution of climate extreme

events. Nat. Clim. Change 5, 725–730.
Vautard, R., Yiou, P., van Oldenborgh, G.-J., Lenderink, G., Thao, S., Ribes, A., Planton, S., Dubuisson, B., Soubeyroux, J.-M., 2015. Extreme fall 2014 precipitation in the Cévennes mountains. Bull. Am. Meteorol. Soc. 96 (12), S56–S60.
Vrac, M., Drobinski, P., Merlo, A., Herrmann, M., Lavaysse, C., Li, L., Somot, S., 2012. Dynamical and statistical downscaling of the French Mediterranean climate: uncertainty assessment. Nat. Hazards Earth Syst. Sci. 12, 2769–2784.
Weedon, G.P., Gomes, S., Viterbo, P., Shuttleworth, W.J., Blyth, E., Österle, H., Adam, J.C., Bellouin, N., Boucher, O., Best, M., 2011. Creation of the WATCH Forcing Data and its use to assess global and regional reference crop evaporation over land during the twentieth century. J. Hydrometeorol. 12, 823–848.